THE JOURNAL OF BIOLOGICAL CHEMISTRY VOL. 285, NO. 25, pp. 19338–19345, June 18, 2010

Structural Basis of the Lactate-dependent Allosteric Regulation of Oxygen Binding in Arthropod Hemocyanin*[S]

Received for publication, October 15, 2009, and in revised form, April 19, 2010 Published, JBC Papers in Press, April 20, 2010, DOI 10.1074/jbc.M109.076067

Shun Hirota[‡1], Naoki Tanaka[‡], Ivan Mičetić[§], Paolo Di Muro[§], Satoshi Nagao[‡], Hiroaki Kitagishi[¶], Koji Kano[¶], Richard S. Magliozzo[‖], Jack Peisach[**], Mariano Beltramini[§], and Luigi Bubacco[§2]

*From the [‡]Graduate School of Materials Science, Nara Institute of Science and Technology, 8916-5 Takayama, Ikoma, Nara 630-0192, Japan, the [§]Department of Biology, University of Padova, I-35121 Padova, Italy, the [¶]Department of Molecular Science and Technology, Faculty of Engineering, Doshisha University, Kyototanabe, Kyoto 610-0321, Japan, the [‖]Department of Chemistry, Brooklyn College, Brooklyn, New York 11210, and the **Department of Physiology and Biophysics, Albert Einstein College of Medicine, Bronx, New York 10461*

Hemocyanin (Hc) is an oxygen carrier protein in which oxygen binding is regulated by allosteric effectors such as H^+ and L-lactate. Isothermal titration calorimetric measurements showed that L-lactate binds to dodecameric and heterohexameric Hc and to the *Cae*SS3 homohexamer but not to the *Cae*SS2 monomer. The binding of lactate caused no change in the optical absorption and x-ray absorption spectra of either oxy- or deoxy-Hc, suggesting that no structural rearrangement of the active site occurred. At pH 6.5, the oxygen binding rate constant k_{obs} obtained by flash photolysis showed a significant increase upon addition of L-lactate, whereas L-lactate addition had little effect at pH 8.3. Lactate binding caused a concentration-dependent shift in the interhexameric distances at pH 6.5 based on small angle x-ray scattering measurements. These results show that L-lactate affects oxygen affinity at pH 6.5 by modulating the global structure of Hc without affecting its binuclear copper center (the active site). In contrast to this, the active site structure of deoxy-Hc is affected by changes in pH (Hirota, S., Kawahara, T., Beltramini, M., Di Muro, P., Magliozzo, R. S., Peisach, J., Powers, L. S., Tanaka, N., Nagao, S., and Bubacco, L. (2008) *J. Biol. Chem.* 283, 31941–31948). Upon addiction of lactate, the kinetic behavior of oxygen rebinding for Hc was heterogeneous under low oxygen concentrations at pH 6.5 due to changes in the T and R state populations, and the equilibrium was found to shift from the T toward the R state with addition of lactate.

Hemocyanin (Hc)[3] is an oxygen carrier protein present in the hemolymph of several arthropod species. Its biological function is based on the reversible binding of molecular oxygen to an active site containing a binuclear copper center (1). Arthropod Hcs are oligomeric proteins comprising 75-kDa subunits, each containing a single active site. In the presence of Ca^{2+} and Mg^{2+} *in vivo* and *in vitro*, the protein exists as heterohexamers (or multiheterohexamers) in which different subunits interact through specific contact areas. In the case of *Carcinus aestuarii* Hc, at least three subunit types (*Cae*SS1, *Cae*SS2, and *Cae*SS3) have been isolated and characterized (2). The subunits within the hexamer are arranged into two layers of trimers which are shifted by 60° relative to one another. One 3-fold symmetry axis exists along the axial direction of the molecule, whereas three 2-fold symmetry axes are oriented perpendicularly to the 3-fold axis (1). Subunit-subunit interactions are responsible for formation of hexamers (1 × 6-mers of 450 kDa) and for the interaction of hexameric building blocks to form 2 × 6- (3), 4 × 6- (4), 6 × 6- (5), and 8 × 6-mers (6) with molecular masses up to millions of daltons. These complex quaternary structures are species-specific, but all oligomers can be dissociated into monomers by removing Ca^{2+} and Mg^{2+} ions and/or increasing pH (3).

At the active site, each copper ion is bound to the imidazole ϵ-nitrogen of three conserved histidine residues. Reversible oxygen binding occurs at this site, and the protein can exist in two forms: deoxygenated (deoxy-Hc) and oxygenated (oxy-Hc), as a function of the oxygen concentration and the presence of allosteric effectors such as hydrogen ions or L-lactate. In the deoxy form, the active site copper is cuprous Cu(I) and the protein is colorless, whereas for the oxygenated form, the active site is formally a Cu(II)-O_2^{2-}–Cu(II) complex and has blue color. Oxygen is bound in the μ-η^2:η^2 mode, and the absorption spectrum of the oxygenated site is characterized by absorption bands at 337 and 560 nm, assigned respectively to $\pi_{\sigma^*} \rightarrow$Cu(II) and $\pi_{v^*} \rightarrow$Cu(II) charge transfer transitions (7).

Hcs bind oxygen cooperatively, and as a general rule, the more complex quaternary structures with higher molecular mass exhibit stronger cooperative interactions manifested in increased Hill coefficients. Investigation of the origins of cooperativity has been approached through examination of the three-dimensional crystal structures of deoxy- and oxy-Hc (8) as well as through x-ray absorption spectroscopy (XAS) (9) and small angle x-ray scattering (SAXS) (10, 11), in some cases in the presence of small molecules acting as allosteric modifiers

* This work was supported by National Institutes of Health Grant GM40168 (to J. P.). This work was also supported by Grants-in-aid for Scientific Research from Ministry of Education, Culture, Sports, Science and Technology, Japan and Japan Society for the Promotion of Science (to S. H.), Fondo per gli Investimenti della Ricerca di Base, Ministero università e ricerca, and "Progetto di Ateneo" CPDA 051777 from the University of Padova (to L. B. and M. B.) and by the Executive Program of Cooperation in the Fields of Science and Technology between the Government of Italy and the Government of Japan (to L. B. and S. H.).
[S] The on-line version of this article (available at http://www.jbc.org) contains supplemental Figs. S1–S9.
[1] To whom correspondence may be addressed. E-mail: hirota@ms.naist.jp.
[2] To whom correspondence may be addressed: Dept. of Biology, University of Padova, Via Ugo Bassi 58B, Padova 35121, Italy. E-mail: luigi.bubacco@unipd.it.
[3] The abbreviations used are: Hc, hemocyanin; deoxy-Hc, deoxygenated Hc; oxy-Hc, oxygenated Hc; XAS, x-ray absorption spectroscopy; SAXS, small angle x-ray scattering; ITC, isothermal titration calorimetry; MES, 4-morpholineethanesulfonic acid; DA model, dummy atom model.

and/or at low pH. The results of these studies indicate conformational changes that occur at the level of the active site as well as the tertiary and quaternary structure of multimers. In particular for the metal site, an important trigger for affinity change is believed to be an alteration in the copper-copper distance reported to be 4.6 Å in deoxy-Hc and 3.6 Å in oxy-Hc (8), whereas the average bond lengths for the N_ϵ-to-copper bonds are essentially unchanged in both forms. Such a rearrangement would enable coordination of dioxygen to both metal ions. Little additional structural information concerning tertiary and quaternary changes accompanying oxygen binding comes from comparison of the crystal structures of the oxy and deoxy subunit II homohexamers from *Limulus polyphemus* (which are noncooperative); in these examples, the tertiary and quaternary structures of oxygenated and deoxygenated hexamers are quite similar (12). Therefore, little insight into the structural origins of cooperativity is currently available. However, structural features at the level of protein subunit interactions must change in native Hcs as a function of ligand binding because there are no direct interactions in the dicopper site with effector molecules such as hydrogen ions or L-lactate, both of which are known to alter oxygen affinity and cooperativity.

Oxygen binding by Hcs is finely regulated by a number of allosteric effectors such as H^+ (9, 13), L-lactate (10), and urate (14). Several models (two-state, three-state, and nested Monod-Wyman-Changeux models) have been applied to describe the binding affinity and cooperativity of arthropod Hcs and their dependence on solution conditions (15). Although allosteric regulators are believed to play important roles *in vivo*, information on the molecular mechanisms that lead to the observed changes in oxygen affinity and cooperativity is scanty. In general, an increase in H^+ concentration decreases oxygen affinity as well as cooperativity (3, 16). This phenomenon is referred to as the Bohr effect. The range of pH values for a strong Bohr effect in decapods is 7.4–7.8, which is the physiologically relevant range for the seawater environment (17). The origin of the effect has been recently interpreted in terms of a protonation-dependent change in the active site geometry of copper, resulting in a change in the binding rate of dioxygen to the dinuclear Cu(I) active site in the subunits (9).

Compared with H^+, L-lactate has an opposite effect such that increasing the L-lactate concentration increases oxygen affinity and cooperativity of binding. L-Lactate is a metabolite generated as a by-product of glycolysis under low oxygen conditions, and its concentration in cells is directly dependent on the oxygen debt. The physiological concentration of L-lactate under normoxia is very low (0.030–0.1 mM) (18, 19), but it can increase up to ~30 mM during high activity of the animal (20). Under these conditions of acidosis, the importance of the L-lactate effect increasing the oxygen affinity could reside in counterbalancing the Bohr effect in Hc thus maintaining the oxygen affinity of the carrier. It had been suggested from oxygen affinity measurements on *Panulirus interruptus* and *Callinectes sapidus* Hc that L-lactate not only shifts the allosteric equilibrium toward the high affinity form (R state) from the low affinity form (T state) of the protein but also increases the oxygen affinity of both the T and R states (21, 22); in contrast to this, a more recent study on *Carcinus maenas* Hc suggested that L-lactate increases oxygen affinity by preferentially raising the oxygen affinity in the T state without affecting the affinity in the R (or high affinity) state (18). Concerning the L-lactate interaction site, L-lactate has been recently shown by electrospray ionization mass spectrometry to interact with the lightest subunits of *C. maenas* Hc (23) at a site or sites only formed in assembled hexamers. Despite the fact that pH and L-lactate affect the oxygen binding characteristics of Hc in a physiologically relevant fashion, their structural effects on Hc are still not defined in detail.

In this paper, we have addressed the issue of the L-lactate effect on oxygen binding mainly in the Hc from the brachyuran crab *C. aestuarii*. We chose this Hc because its oxygen-binding behavior has been investigated in detail as a function of both pH and L-lactate concentration (9, 18). Isothermal titration calorimetry (ITC) experiments were performed to monitor L-lactate binding to the protein, optical and XAS were applied to characterize structural effects on the active site, and flash photolysis was used to define the rate constants for oxygen binding under various conditions. Finally, SAXS was used to disclose conformational effects at the level of tertiary and quaternary structures. The results provide new insights into the physiology of Hc function and how L-lactate affects oxygen binding affinity by modulating the global structure of the protein without affecting its active site.

EXPERIMENTAL PROCEDURES

Preparation of Hc Samples—Hc was purified from the hemolymph of live animals as described previously (2, 24). The protein was purified to a final concentration of 25 mg/ml in 50 mM Tris-HCl, pH 7.6, with 20 mM $CaCl_2$ and stored at −20 °C with 20% sucrose added as a cryoprotectant. Sucrose was eliminated before the measurements by overnight dialysis against the chosen buffer. The Hc obtained resulted in a mixture of ~18% hexameric and 82% dodecameric fractions (supplemental Fig.S1). The dodecameric fraction was purified from the mixture by size exclusion chromatography on a Pharmacia fast protein liquid chromatography system (SEC-FPLC) with a prep-grade Hi-Load Superdex 200 26/60 column (Pharmacia) equilibrated with the same buffer. The dodecameric fraction did not dissociate further, and its oxygenation state was estimated from the absorbance ratio A_{337}/A_{278}, assuming 0.21 for a fully oxygenated form (2). The *Cae*SS2 and *Cae*SS3 monomers were purified as described previously (2). The isolated *Cae*SS3 monomers were then converted to homohexamers by addition of 20 mM $CaCl_2$ at pH 7.6. It is worth mentioning that the *Cae*SS2 monomer does not assemble into higher molecular mass species (2).

ITC Measurements—Microcalorimetric measurements were carried out on purified dodecameric *C. aestuarii* Hc, its *Cae*SS2 monomer, and *Cae*SS3 homohexamer with a VP-ITC isothermal titration calorimeter (MicroCal). Titration curves were obtained at 20 °C by adding 25 aliquots (10 μl each) of L-lactate (100 mM) into Hc (1.453 ml, 16.7 μM hexamer) using buffers of 50 mM MES-NaOH, pH 6.5, or 50 mM Tris-HCl, pH 8.3, each with 20 mM $CaCl_2$. The titration curves were measured several times for each condition and analyzed with the ORIGIN software program.

Optical Absorption Measurements—Optical absorption spectra were measured at 37 °C on a Shimadzu UV-3100PC spectrophotometer. The protein concentration was adjusted to 80 μM (subunit) in 50 mM Tris-HCl or MES-NaOH buffer, each containing 20 mM $CaCl_2$ at the desired pH.

X-ray Absorption Measurements—CuK-edge absorption spectroscopy was carried out on highly concentrated (1 mM subunits, *i.e.* 2 mM in copper) Hc solutions on beam lines X-9A and X-10C at the National Synchrotron Light Source (NSLS), Brookhaven National Laboratory. Sample handling, radiation flux, scanning, and signal detection as well as data analysis were performed as described previously (9).

Flash Photolysis Measurements—Purified *C. aestuarii* Hc, *Cae*SS2 monomer, and *Cae*SS3 homohexamer in 50 mM Tris-HCl, pH 8.3, each with 20 mM $CaCl_2$, were degassed on a vacuum line and then flushed with nitrogen gas. Dithionite was added anaerobically (final concentration 1 mM) to reduce any cupric copper in the protein. The solution was then dialyzed under aerobic conditions against 50 mM Tris-HCl or MES with 20 mM $CaCl_2$ at the desired pH. After dialysis, the protein concentration was adjusted to 20 μM (subunit), and the sample was equilibrated under an atmosphere of oxygen plus nitrogen, prepared using a gas generator (MX-3S; Crown, Tokyo, Japan), such that the partial pressure of oxygen varied from 5 to 100%. The sample solution was transferred into a sealed quartz cell, which was filled with the same gas mixture. Photolysis of oxy-Hc samples was accomplished using the third harmonic of a Nd:YAG laser (Surelight I-10; Continuum, Santa Clara, CA; pulse energy, 40 mJ; pulse width, 5 ns; pulse frequency, 10 Hz) for excitation. Time-resolved absorbance changes were measured at 20 °C with illumination from a xenon lamp orthogonal to the laser pulse and were recorded on a digital oscilloscope (TDS 3012B; Tektronix, Tokyo, Japan), which received voltage signals from the photomultiplier attached to a monochromator (RSP-601-03; Unisoku, Osaka, Japan). The traces were obtained as averages of 512 or 640 pulses, and least squares exponential fits were performed for the time-resolved absorption data using Igor Pro version 6.0 (WaveMetrics).

SAXS—SAXS measurements were carried out at the SOLEIL synchrotron (St. Aubin, France), beamline SWING. The wavelength of the monochromatic x-ray beam was 1.033 Å, and the scattering pattern was recorded on a two-dimensional CCD camera. The sample-to-detector distance was 2.3 m, giving a scattering vector q range of 0.01 to 0.3Å^{-1} ($q = 4\pi^*\sin(\theta)/\lambda$ with 2θ as scattering angle). *C. aestuarii* Hc was present in the samples as a mixture of hexamers and dodecamers (supplemental Fig. S1). Fully oxygenated samples were measured at a concentration of 4 mg/ml in 50 mM MES, pH 6.5, and 50 mM Tris-HCl, pH 8.3, with 20 mM $CaCl_2$ in the presence of the reported L-lactate concentrations. Exposure time was 4 s, and typically 15 exposures for protein and 20 exposures for buffer samples were averaged. No radiation damage effects in terms of oxygen binding properties and protein cleavage could be detected subsequent to x-ray exposure. Raw experimental scattering curves were normalized for detector response, photon flux, and capillary thickness. Buffer-subtracted curves were analyzed with GNOM (25) and yielded particle distance distribution functions $p(r)$, maximum particle dimensions, and particle radii of gyration. *Ab initio* shape determination of *C. aestuarii* Hc was carried out using the dummy atom (DA) method as implemented in the program DAMMIF (26, 27). Such models are defined as an assembly of densely packed spheres with radii much smaller than the maximum particle dimension. Because of the stochastic nature of the DA optimization algorithm, several runs of the program were performed to obtain an acceptable solution. 700 DA models were obtained from the scattering curves under all six conditions analyzed (at pH 6.5 and 8.3 and L-lactate concentrations of 0, 1, and 40 mM). Of the 700 DA models, approximately 50–60% were not acceptable because they presented small, loosely connected or poorly defined DA "domains." The selection of the DA model was done by first computing a tight boundary around each DA model using principal components analysis (28) and then removing the DA models that presented an increase in one of the bounding-box lengths of more than 2 to 5% from the average value. For each accepted DA model, dummy atoms were clustered in two groups (each group representing a single hexamer), and the center of each cluster was calculated from the mean of the DA coordinates that belong to the cluster. The interhexameric separation was then calculated as a geometric distance between the cluster centers.

RESULTS

ITC Measurements of Lactate Binding to Hc—To obtain information on the binding of L-lactate to Hc, ITC measurements were performed using purified *C. aestuarii* Hc at pH 6.5 and 8.3 and *Cae*SS2 monomer at pH 6.5 (Fig. 1). The titration of purified *Cae*SS3 homohexamers prepared from reassociated monomers was also obtained (supplemental Fig. S2). Previous L-lactate titration studies of *C. sapidus* Hc reported 2.2 binding sites/hexamer, and ultrafiltration techniques gave 2.8 sites/hexamer (29). However, the same authors reported approximately one binding site of L-lactate for *P. interruptus* Hc hexamer based on oxygen equilibrium studies (21). Recently, a mole ratio of 0.35 L-lactate per subunit was reported for *C. meanas* Hc (hemolymph) at pH 7.0 (18).

In the current study, L-lactate binding showed a typical curve for 1:1 binding to the hexameric Hc with a binding constant of about 840 ± 30 M^{-1} at pH 8.3. The ΔH and ΔS obtained from the fitting were −40 ± 4 kJ/mol and −80 ± 20 J/(K·mol), respectively. For titration of L-lactate at pH 6.5, the fitting of the data with a model of 1:1 stoichiometry was not as successful as that obtained for pH 8.3. A two-site fitting was therefore used that provided two binding constant values of about 840 ± 140 and 65 ± 35 M^{-1}, respectively. The ΔH and ΔS of each phase were −30 ± 5 kJ/mol, −50 ± 10 J/(*K*·mol) and −32 ± 4 kJ/mol, −75 ± 30 J/(*K*·mol), respectively. The binding constant for the weak phase was comparable with that obtained by the flash photolysis experiments (described below). No binding of lactate by titration of *Cae*SS2 monomer subunits at pH 6.5 could be demonstrated whereas binding was found in the case of the *Cae*SS3 homohexamer; these results are in agreement with flash photolysis data (see below) showing that L-lactate had no effect on the value of k_{obs} for the *Cae*SS2 monomer, whereas an effect was demonstrated for the *Cae*SS3 homohexamer.

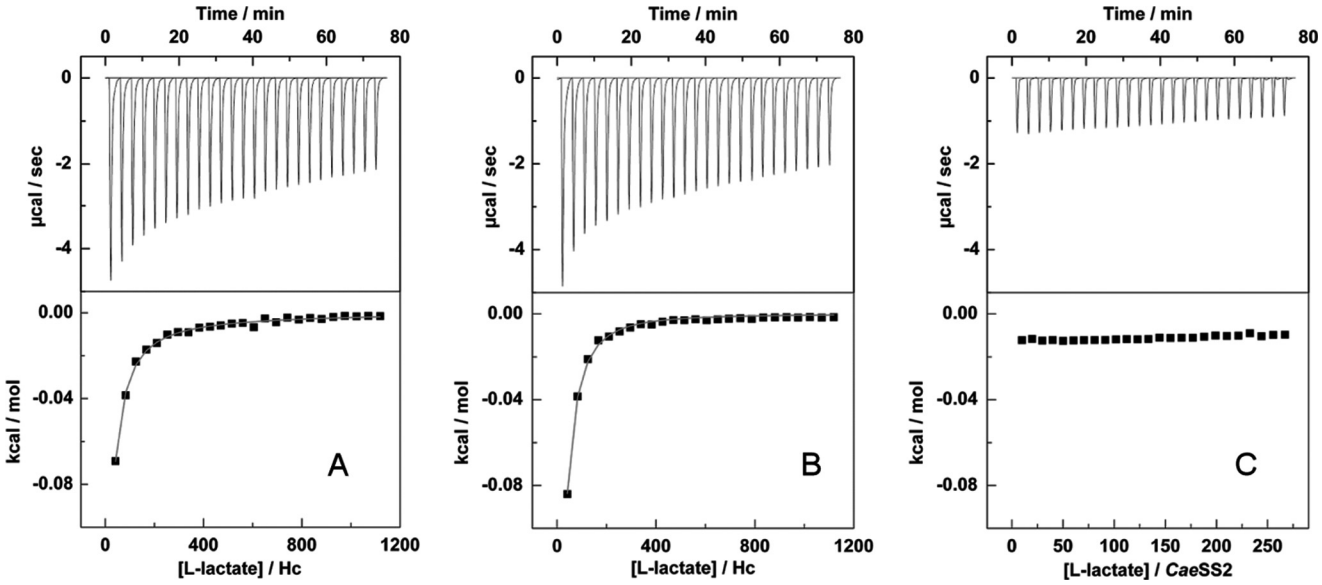

FIGURE 1. **Calorimetric titration of *C. aestuarii* oxy-Hc (16.7 μM hexamer) with successive injections of L-lactate (100 mM in the syringe, 25 × 10-μl aliquots) at pH 6.5 (*A*) and 8.3 (*B*) together with titration of *Cae*SS2 monomer (70 μM) at pH 6.5 (*C*).** *Upper*, raw data showing the amount of heat generated after each injection of L-lactate. *Lower*, plot of the amount of heat generated per injection as a function of the L-lactate/Hc molar ratio. The *solid lines* represent the best-fitted curves of the data to a model of hexamer:L-lactate = 1:2 (*A*) and 1:1 (*B*) stoichiometry, respectively. Titration of the ligand without the protein was performed to subtract the effect of the heat because of ligand dilution.

L-Lactate Binding Does Not Affect the Binuclear Copper Site—After establishing that L-lactate binds to oligomeric Hc in a physiologically relevant range of concentrations, the 560 nm charge transfer band in the optical spectrum of oxy-Hc was used as a spectroscopic probe to explore the effect of L-lactate on the integrity of the binuclear copper center. As shown in supplemental Fig. S3, the optical properties of oxy-Hc are not affected by L-lactate, either at pH 6.5 or 8.3.

The optical results were confirmed by XAS. This technique is a sensitive probe of the electronic structure of the copper ions and the geometry of the active site. The edge spectra of oxygenated *P. interruptus* Hc in the presence and absence of L-lactate were almost superimposable (supplemental Fig. S4). However, under the same conditions the oxygen-binding rate constant k_{obs} (defined in the following paragraph) at pH 7.3 under oxygen saturation increased from 42.7 ± 1.4 to 47.2 ± 0.5 ms^{-1}. Additionally, XAS provides a unique approach to investigate the deoxy-Hc active site which is not amenable to other spectroscopic tools because of the electronic structure of Cu(I). Clearly resolved changes were reported previously for the effects of hydrogen ions on the structure of the deoxy-Hc copper center (9). However, spectra of deoxy-Hc with and without L-lactate (up to the same amount used for the ITC measurements) were very similar (supplemental Fig. S5). These observations show that the oxy and deoxy forms of Hc do not undergo detectable structural rearrangement of the active site upon L-lactate binding to the protein.

Kinetics of Oxygen Rebinding after Photodissociation of Oxy-Hc—The irradiation of oxy-Hc with laser pulses at 355 nm results in the photolysis of bound oxygen to give the deoxy protein, followed by ligand rebinding after the pulse. Because of the spectroscopic difference between oxy- and deoxy-Hc, the first step (photolysis) decreases the intensity of the 337 nm absorption band. Under the conditions used here for photolysis, this decrease was less than 5% of the change that occurs upon complete deoxygenation, indicating that only a small fraction of the protein was converted. Throughout the photolysis experiment the Hc multimers remain in the high affinity form. After photolysis, oxygen rebinding can be followed by the absorption increase at 337 nm on a time scale of 10 μs to 1 ms, and the oxygen-binding rate constant, k_{obs}, is obtained by single-exponential fitting of the kinetic data. The initial absorption intensity is restored at the end of the rebinding process demonstrating the full reversibility of the photolysis. The correlation of the observed effect with the expected optical changes of the oxy-Hc active site had been demonstrated in a previous study showing that the action spectrum for photolysis strictly follows the absorption band of oxy-Hc (9).

The pH dependence of k_{obs} under oxygen saturated conditions (1.39 mM) in the presence and absence of 40 mM L-lactate is shown in Fig. 2. The sigmoidal behavior of k_{obs} in the absence of L-lactate shows that there are two states for Hc, corresponding to the species present at high and low pH values. The pK_a for conversion between these two states was about 7.6 and was not affected by the addition of L-lactate. At low pH (pH 6.5), the k_{obs} value showed a significant increase upon the addition of L-lactate, whereas at high pH (pH 8.3) L-lactate addition had little effect. A pH dependence of k_{obs} was also found in the case of the *Cae*SS2 monomer, whereas L-lactate had no influence on oxygen binding properties (Fig. 2). On the other hand, the k_{obs} for oxygen rebinding to the *Cae*SS3 homohexamer at pH 6.5 under oxygen saturated conditions increased from 73.6 ± 0.7 to 82.8 ± 0.7 ms^{-1} with addition of 40 mM L-lactate.

Oxygen rebinding kinetic experiments were performed at pH 6.5 and 8.3 as a function of oxygen concentration, yet exploring a range of values that ensure full saturation of Hc with oxygen before photolysis in each case. The k_{obs} values increased linearly as a function of oxygen concentration (supplemental Fig. S5) as

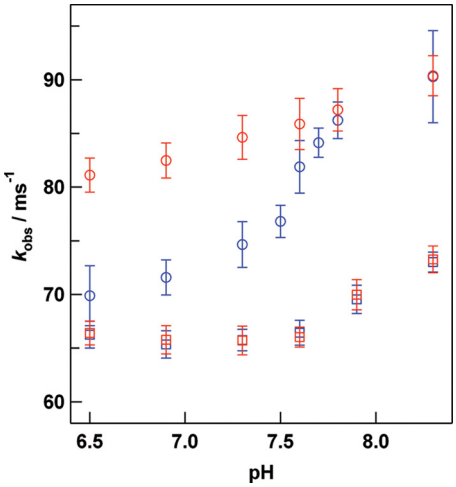

FIGURE 2. **pH dependence of k_{obs} for oxygen rebinding to the dodecameric form of *C. aestuarii* Hc (*circles*) and *Cae*SS2 monomer (*squares*) in the presence (*red*) and absence (*blue*) of 40 mM L-lactate.** Experimental conditions: 20 μM (subunit) Hc; 1.39 mM O_2; laser pulse, 40 mJ, 10 Hz; 20 °C. Each *trace* is an average of 64 × 8 or 64 × 10 shots.

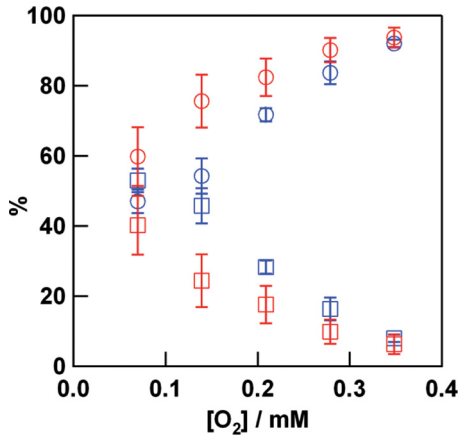

FIGURE 3. **Percentage of the fast (*circles*) and slow (*squares*) phases of oxygen rebinding obtained by flash photolysis of *C. aestuarii* oxy-Hc in the presence (*red*) and absence (*blue*) of 40 mM L-lactate under various oxygen concentrations at pH 6.5.** Least square fitting of the time course of the absorption change was performed. Experimental conditions are the same as those in Fig. 2, except for a higher Hc concentration (60 μM subunit) for the experiment under 5% oxygen and 95% nitrogen atmosphere, for which results were essentially the same as that obtained for 20 μM (subunit) Hc.

expected for a simple rebinding phenomenon. The increase was observed for the oxygen concentrations investigated, both at pH 6.5 and 8.3, as well as in the presence and absence of L-lactate. From these plots, k_{on} and k_{off} can be calculated using Equation 1 (9).

$$k_{obs} = k_{on}([\text{deoxy-Hc}] + [O_2]) + k_{off} \qquad \text{(Eq. 1)}$$

Under our experimental conditions, oxygen is in large excess with respect to Hc (at 20 °C, $[O_2]$ = 220 μM, $[Hc]_{total}$ (subunit) = 20 μM; <5% of Hc becomes deoxygenated after photoreaction), hence the term [deoxy-Hc] can be neglected in Equation 1, and the observed rebinding rate depends linearly on the oxygen concentration. The observed oxygen binding rate increased with increasing pH from 6.5 to 8.3 for all oxygen concentrations investigated. At pH 8.3, the k_{obs} values in the presence and absence of L-lactate were essentially the same (supplemental Fig. S6, *triangles*). These results indicate that k_{on}, k_{off}, and thus the dissociation constant K_D are not affected by L-lactate at pH 8.3 within the investigated oxygen concentrations where the protein is largely in the high affinity form.[4] In contrast, at pH 6.5 the k_{obs} value increases upon addition of L-lactate. The plot of k_{obs} *versus* $[O_2]$ had a steeper slope and the same intercept, indicating an increase in k_{on} and K_D values in the presence of L-lactate (supplemental Fig. S6). The value of k_{obs} for oxygen binding to Hc at pH 6.5 with various L-lactate concentrations under oxygen-saturated conditions showed characteristic saturation behavior (supplemental Fig. S7). The change in k_{obs} as a function of L-lactate concentration at pH 6.5 was fitted well by assuming a 1:1 complex of the hexamer and L-lactate. The binding constant was estimated by least squares fitting to be 160 ± 70 M^{-1}. Because it is known that two lactate molecules can bind per hexamer, as shown by previous reports (21, 29) and here using calorimetry at pH 6.5, the lactate dependence of k_{obs} corresponds to that for the lower affinity binding.

Flash photolysis experiments carried out under low oxygen concentrations (5% oxygen and 95% nitrogen at atmospheric pressure) at pH 6.5 revealed heterogeneity in the kinetic behavior of oxygen rebinding. The protein is still multimeric under these conditions, and thus the recovery of the absorption at 337 nm is fitted by a double, rather than a single exponential (9). The contribution from the slower phase compared with that of the faster phase increases as the oxygen concentration is decreased (Fig. 3). The amplitude of the two phases was comparable under 5% oxygen atmosphere at pH 6.5, whereas the fast phase becomes predominant upon increasing the oxygen concentration. The fast and slow phases may be attributed to oxygen binding to R and T state multimers, respectively. The amplitude of the fast phase increases at all oxygen concentrations in the presence of L-lactate. A shift from the T toward the R state by addition of lactate is consistent with a previous report for *C. sapidus* Hc (22). In contrast to the behavior of the multimeric protein, the oxygen rebinding for *Cae*SS2 monomer shows a single phase even at low oxygen and low pH conditions (supplemental Fig. S8).

SAXS—SAXS data (supplemental Fig. S9) were analyzed according to standard procedures to generate the distance distribution function $p(r)$, which represents the probability of finding two volume elements separated by distance r within the population of observed scattering centers. The $p(r)$ function represents a histogram of all distances in the sample, thus it gives information about particle shape and changes that the molecule undergoes under different conditions. As previously observed for *Homarus americanus* Hc (10), the $p(r)$ curve of the 2 × 6-meric *C. aestuarii* Hc is composed of two overlapping bell-shaped curves. The first one with the maximum around 75 Å reflects the distance distribution of volume elements within the hexamers, whereas the second curve around 140 Å, reflects interhexameric distances.

[4] An effect of L-lactate on the low affinity form has been described at pH 7.85 in Ref. 18, but the effect occurs under low saturation conditions where the amount of oxygenated protein would be below the optical absorbance detection limit in the flash photolysis experiment.

Because only small differences were observed upon the addition of L-lactate, the effect of L-lactate on *C. aestuarii* Hc was further evaluated by using a novel approach that involves calculating the interhexameric distances of all DA models fitted to the scattering data. Following the removal of poor DA models, interhexameric distances were compared using *t* test statistics. Interestingly, there was no significant difference in the distribution of interhexameric distances between the samples at pH 6.5 and 8.3. Upon addition of L-lactate, the low pH sample had a lactate concentration-dependent shift toward larger interhexameric distances whereas the high pH sample showed an opposite trend (smaller interhexameric distance with increasing L-lactate). The comparison between histograms of interhexameric distances obtained from DA models is shown in Fig. 4. These results show that the structural changes induced in the quaternary structure of Hc by interaction with L-lactate are opposite at high and low pH.

DISCUSSION

pH Effect on Hc Structure—The structural basis of the pH effect on the oxygen binding properties of Hc (the Bohr effect) and the effect on the rate constants obtained in flash photolysis experiments have been reported previously (9). In that study, the k_{on} value increased when the pH was raised from 6.5 to 8.3 (pH 6.5, 49.1 ± 0.6 $mM^{-1}s^{-1}$; pH 8.3, 63.5 ± 0.5 $mM^{-1}s^{-1}$). These results show that the oxygen binding rate constant of deoxy-Hc sites in the high affinity form of the multimeric protein, which is present because nearly all sites retain oxygen in the photolysis experiment, increased with increasing pH, whereas no significant change was observed for the k_{off} value. In another related type 3 copper protein, the bacterial phenol and cathecol oxidase tyrosinase which is monomeric, no significant pH dependence was observed in its oxygen binding, which shows that the pH dependence in Hc is a characteristic that emerged in oligomeric Hcs (30). From the oxygen-binding rate constants reported here, the pH dependence in the R state (the high affinity form) exhibited a pK_a value of 7.6, which was not affected by the presence of L-lactate. Therefore, at least two substates should exist for the high affinity form of oxy-Hc (at high oxygen concentration), R (low pH) and R* (high pH). This is consistent with a prior report that hydrogen ions cause structural changes in the active site of deoxy-Hc (9).

Beyond the previously reported pH-dependent geometry of copper in the deoxy protein, the Bohr effect could also arise from changes in structural features remote from the active site. The data presented here, however, do not provide any evidence for a role of the quaternary structure in the Bohr effect. This is based on three independent observations. Variation of pH does not affect the equilibrium between hexamers and dodecamers (supplemental Fig. S9). The quaternary structures of the dodecamers at low and high pH values were indistinguishable in the SAXS analysis of the interhexameric distances. Finally, the k_{obs} for the *Cae*SS2 monomer increased at higher pH (Fig. 2). Taken together, these results indicated that the Bohr effect depends upon local effects on the structure of the active site.

L-Lactate Binding to Hc—Microcalorimetric results showed that L-lactate binds to Hc with an affinity consistent with physiological relevance (binding constant about 840 M^{-1}), but at

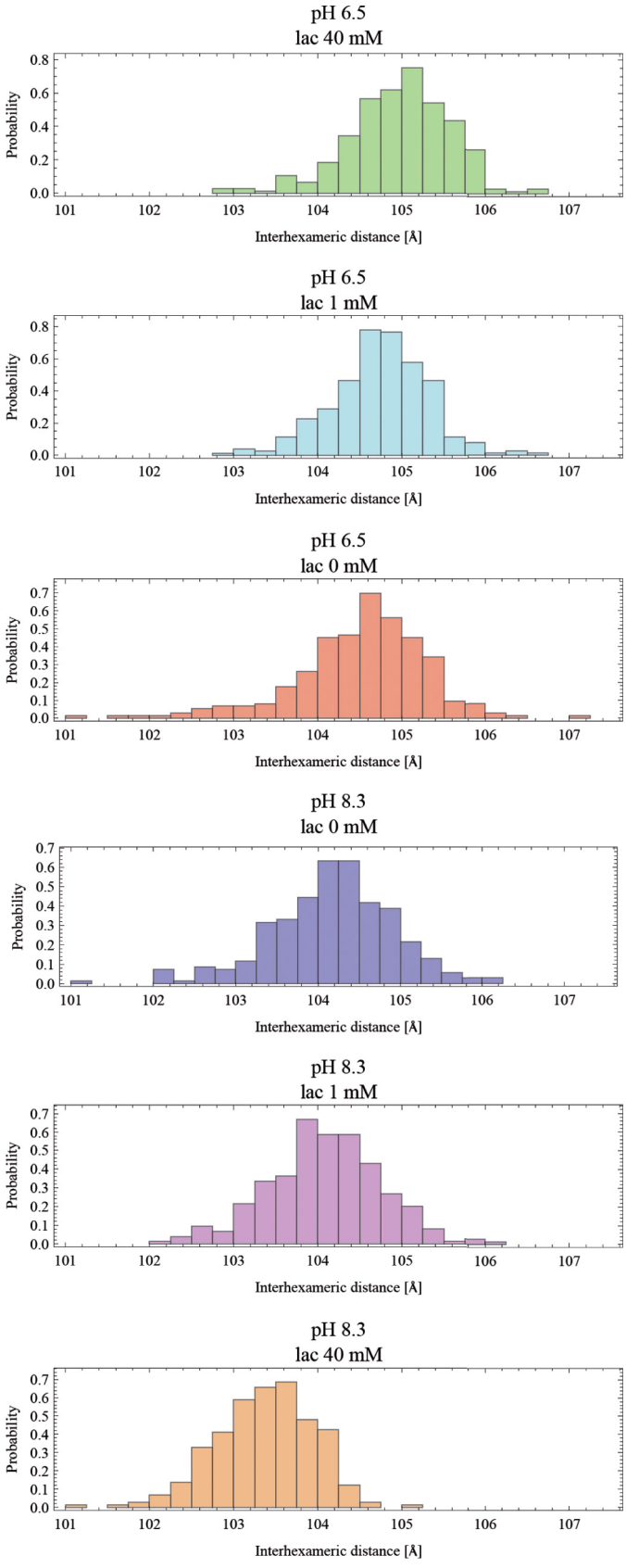

FIGURE 4. **Histogram of interhexameric distance distributions in *C. aestuarii* Hc as calculated from DA models generated by multiple runs of the DAMMIF program.** *Red*, pH 6.5, 0 mM L-lactate; *light blue*, pH 6.5, 1 mM L-lactate; *green*, pH 6.5, 40 mM L-lactate; *blue*, pH 8.3, 0 mM L-lactate; *purple*, pH 8.3, 1 mM L-lactate; *orange*, pH 8.3, 40 mM L-lactate.

high pH, the protein exhibits the same oxygen binding properties with or without this effector. A second binding process for L-lactate was found to have a binding constant of 65 ± 35 M^{-1}. This phase was detected by calorimetric experiments at pH 6.5 but not at pH 8.3. The binding constant of 65 ± 35 M^{-1} was comparable with the value obtained from the modulation of the oxygen binding constant by L-lactate observed in the flash photolysis experiments (160 ± 70 M^{-1}). Here, the low affinity binding constant for lactate was observed only at pH 6.5.

ITC experiments using *Cae*SS3 homohexamers showed that L-lactate binds (and an increased oxygen binding rate constant was found in photolysis experiments), whereas ITC with *Cae*SS2 monomers did not demonstrate any binding, nor does lactate affect the rate of oxygenation in photolysis measurements within the pH range investigated. These data indicate that the hexameric quaternary structure is essential for both L-lactate binding and modification of the oxygen binding affinity.

The structure of the active site of Hc either in the oxy or deoxy state is not substantially changed by the addition of L-lactate. These results suggest that L-lactate likely affects the quaternary structure and thereby modulates oxygen binding properties. This interpretation is supported by the SAXS data that identify a rearrangement of the quaternary structure upon L-lactate addition. The nature of the allosteric effect produced by L-lactate is consequentially distinct from that found in the Bohr effect, in which alteration of the active site structure governs the functional effect (9). Hc is shown to bind only one or two L-lactate molecules/hexamer (21, 29). Because L-lactate affected the oxygen binding rate k_{obs} without affecting the active site structure, this effector likely binds at a remote site and has an indirect (or steric) effect on oxygen binding. Relevant to this is a proposal, a specific phenylalanine near the active site and conserved in Hcs could act as the trapdoor for an oxygen entry/exit channel in Hc (8). This "door" is reported to be open in the *Panulirus* deoxy-Hc x-ray structure and closed in both the oxy and deoxy *Limulus* structures. The authors go on to say that there is an allosterically controlled gating mechanism underlying the function of this phenylalanine in oxygen binding. This type of structural feature could be relevant to the model proposed here in which polypeptide structural changes are concluded to control ligand access to the active site.

In addition, the k_{obs} value for O_2 binding was affected by L-lactate for the *Cae*SS3 homohexamer, which was competent to bind this ligand presumably at an intersubunit site (supplemental Fig. S2). An intersubunit region is the more likely site for L-lactate binding because such binding could induce changes in quaternary structure of the hexameric and/or dodecameric Hc, which would not be expected were lactate to bind to an exterior site.

In conclusion, a scheme that explains the Bohr and L-lactate effects can be developed according to the present results and a previous study of arthropod Hc (9) (Fig. 5). Two structural features are incorporated in the scheme. Rearrangement of the active site with increasing pH, represented by R and R*, and a quaternary structural change caused by L-lactate at pH 6.5 (R *versus* R_{LL}) both produce faster oxygen binding (9) and a shift in

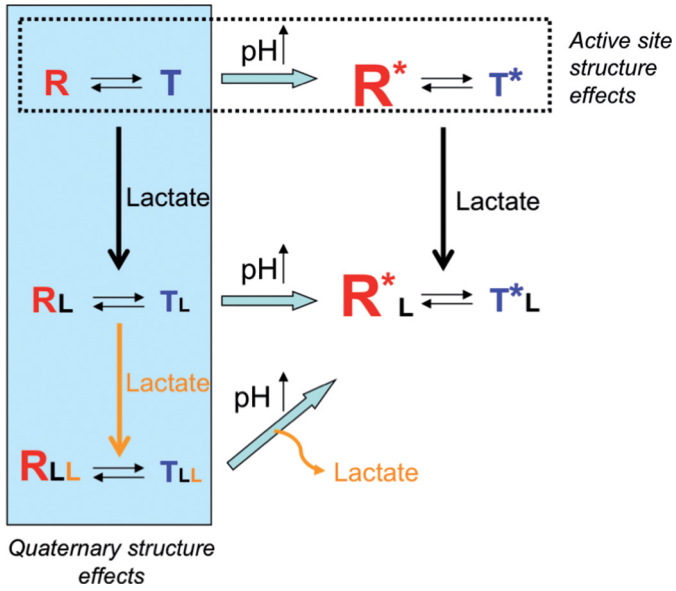

FIGURE 5. **Schematic representation of the pH and L-lactate effects on the structure-function relationships in Hc.** The effect of pH is illustrated *horizontally* across the *top* of the scheme, whereas the effect of increasing L-lactate concentration is shown *vertically* on the *left side*. The size of the letters *R* and *T* represents the amount of these forms. The *R** and *R* represent the two high affinity forms at high and low pH, respectively.

the R-T equilibrium toward the R state. Unlike the affect of pH on active site structure of deoxy-Hc, the effector properties of lactate are mediated through structural changes that do not alter the coordination geometry of the metal ions in the active site.

REFERENCES

1. Volbeda, A., and Hol, W. G. (1989) *J. Mol. Biol.* **209,** 249–279
2. Dainese, E., Di Muro, P., Beltramini, M., Salvato, B., and Decker, H. (1998) *Eur. J. Biochem.* **256,** 350–358
3. Markl, J., and Decker, H. (1992) *Adv. Comp. Environ. Physiol.* **13,** 325–376
4. Cong, Y., Zhang, Q., Woolford, D., Schweikardt, T., Khant, H., Dougherty, M., Ludtke, S. J., Chiu, W., and Decker, H. (2009) *Structure* **17,** 749–758
5. Markl, J., Moeller, A., Martin, A. G., Rheinbay, J., Gebauer, W., and Depoix, F. (2009) *J. Mol. Biol.* **392,** 362–380
6. Martin, A. G., Depoix, F., Stohr, M., Meissner, U., Hagner-Holler, S., Hammouti, K., Burmester, T., Heyd, J., Wriggers, W., and Markl, J. (2007) *J. Mol. Biol.* **366,** 1332–1350
7. Metz, M., and Solomon, E. I. (2001) *J. Am. Chem. Soc.* **123,** 4938–4950
8. Magnus, K. A., Hazes, B., Ton-That, H., Bonaventura, C., Bonaventura, J., and Hol, W. G. J. (1994) *Proteins* **19,** 302–309
9. Hirota, S., Kawahara, T., Beltramini, M., Di Muro, P., Magliozzo, R. S., Peisach, J., Powers, L. S., Tanaka, N., Nagao, S., and Bubacco, L. (2008) *J. Biol. Chem.* **283,** 31941–31948
10. Hartmann, H., Lohkamp, B., Hellmann, N., and Decker, H. (2001) *J. Biol. Chem.* **276,** 19954–19958
11. Hartmann, H., and Decker, H. (2002) *Biochim. Biophys. Acta* **1601,** 132–137
12. Hazes, B., Magnus, K. A., Bonaventura, C., Bonaventura, J., Dauter, Z., Kalk, K. H., and Hol, W. G. (1993) *Protein Sci.* **2,** 597–619
13. Decker, H., and Sterner, R. (1990) *J. Mol. Biol.* **211,** 281–293
14. Menze, M. A., Hellmann, N., Decker, H., and Grieshaber, M. K. (2000) *Biochemistry* **39,** 10806–10811
15. Beltramini, M., Colangelo, N., Giomi, F., Bubacco, L., Di Muro, P., Hellmann, N., Jaenicke, E., and Decker, H. (2005) *FEBS J.* **272,** 2060–2075
16. Truchot, J. P. (1992) *Adv. Comp. Environ. Physiol.* **12,** 377–410
17. Mangum, C. P., and Shick, J. M. (1972) *Comp. Biochem. Physiol. B.* **42A,** 693–697

18. Weber, R. E., Behrens, J. W., Malte, H., and Fago, A. (2008) *J. Exp. Biol.* **211,** 1057–1062
19. Lallier, F., and Truchot, J. P. (1989) *Respir. Physiol.* **77,** 323–336
20. Dissanayake, A., Galloway, T. S., and Jones, M. B. (2008) *Marine Environ. Res.* **66,** 445–450
21. Johnson, B. A., Bonaventura, J., and Bonaventura, C. (1987) *Biochim. Biophys. Acta* **916,** 376–380
22. Johnson, B. A., Bonaventura, C., and Bonaventura, J. (1988) *Biochemistry* **27,** 1995–2001
23. Bruneaux, M., Terrier, P., Leize, E., Mary, J., Lallier, F. H., and Zal, F. (2009) *Proteins* **77,** 589–601
24. Bubacco, L., Magliozzo, R. S., Beltramini, M., Salvato, B., and Peisach, J. (1992) *Biochemistry* **31,** 9294–9303
25. Svergun, D. I. (1992) *J. Appl. Crystallogr.* **25,** 495–503
26. Svergun, D. I. (1999) *Biophys. J.* **76,** 2879–2886
27. Franke, D., and Svergun, D. I. (2009) *J. Appl. Crystallogr.* **42,** 342–346
28. Dimitrov, D., Knauer, C., Kriegel, K., and Rote, G. (2009) *Comp. Geom. Theor. Appl.* **42,** 772–789
29. Johnson, B. A., Bonaventura, C., and Bonaventura, J. (1984) *Biochemistry* **23,** 872–878
30. Hirota, S., Kawahara, T., Lonardi, E., de Waal, E., Funasaki, N., and Canters, G. W. (2005) *J. Am. Chem. Soc.* **127,** 17966–17967